0026-895X/10/7703-368–377$20.00
MOLECULAR PHARMACOLOGY
Copyright © 2010 The American Society for Pharmacology and Experimental Therapeutics
Mol Pharmacol 77:368–377, 2010

Vol. 77, No. 3
57513/3563202
Printed in U.S.A.

Simple 2,4-Diacylphloroglucinols as Classic Transient Receptor Potential-6 Activators—Identification of a Novel Pharmacophore

K. Leuner, J. H. Heiser, S. Derksen, M. I. Mladenov, C. J. Fehske, R. Schubert, M. Gollasch, G. Schneider, C. Harteneck, S. S. Chatterjee, and W. E. Müller

Institute of Pharmacology, Biocenter Niederursel, Goethe University, Frankfurt am Main, Germany (K.L., J.H.H., C.J.F., W.E.M.); Institute for Organic Chemistry and Chemical Biology, Frankfurt am Main, Germany (S.D., G.S.); Cardiovascular Physiology, Centre for Biomedicine and Medical Technology Mannheim, Ruprecht-Karls-University Heidelberg, Mannheim, Germany (M.I.M., R.S.); Institute of Biology, Faculty of Natural Sciences and Mathematics, "Sts. Cyril and Methodius," University of Skopje, Skopje, Macedonia (M.I.M.); Charité University Medicine, Section Nephrology/Intensive Care, Campus Virchow, and Experimental and Clinical Research Center, Berlin, Germany (M.G.); Molecular Pharmacology and Cell Biology, Charité, Berlin (C.H.); Institute of Pharmacology and Toxicology & Interfaculty Centre for Pharmacogenomics and Drug Research, Eberhard-Karls-University, Tübingen, Germany (C.H.); and Dr. Willmar Schwabe GmbH & Co. KG Pharmaceuticals, Karlsruhe, Germany (S.S.C.)

Received May 5, 2009; accepted December 10, 2009

ABSTRACT

The naturally occurring acylated phloroglucinol derivative hyperforin was recently identified as the first specific canonical transient receptor potential-6 (TRPC6) activator. Hyperforin is the major antidepressant component of St. John's wort, which mediates its antidepressant-like properties via TRPC6 channel activation. However, its pharmacophore moiety for activating TRPC6 channels is unknown. We hypothesized that the phloroglucinol moiety could be the essential pharmacophore of hyperforin and that its activity profile could be due to structural similarities with diacylglycerol (DAG), an endogenous nonselective activator of TRPC3, TRPC6, and TRPC7. Accordingly, a few 2-acyl and 2,4-diacylphloroglucinols were tested for their hyperforin-like activity profiles. We used a battery of experimental models to investigate all functional aspects of TRPC6 activation, including ion channel recordings, Ca^{2+} imaging, neurite outgrowth, and inhibition of synaptosomal uptake. Phloroglucinol itself was inactive in all of our assays, which was also the case for 2-acylphloroglucinols. For TRPC6 activation, the presence of two symmetrically acyl-substitutions with appropriate alkyl chains in the phloroglucinol moiety seems to be an essential prerequisite. Potencies of these compounds in all assays were comparable with that of hyperforin for activating the TRPC6 channel. Finally, using structure-based modeling techniques, we suggest a binding mode for hyperforin to TRPC6. Based on this modeling approach, we propose that DAG is able to activate TRPC3, TRPC6, and TRPC7 because of higher flexibility within the chemical structure of DAG compared with the rather rigid structures of hyperforin and the 2,4-diacylphloroglucinol derivatives.

Hyperforin is the main active ingredient of St. John's wort, which has been used for centuries to treat depression (Linde et al., 2008). Like most synthetic antidepressants, hyperforin inhibits synaptic reuptake of serotonin and norepinephrine (Müller, 2003; Treiber et al., 2005). Hyperforin is an acylated bicyclic phloroglucinol derivative with little structural and functional resemblances with any known therapeutically used antidepressants. Thus, unlike conventionally known antidepressants, hyperforin is not a competitive inhibitor of neurotransmitter transporters, and it inhibits synaptic neurotransmitter reuptake by elevating intracellular sodium concentrations (Singer et al., 1999; Wonnemann et al., 2000).

The authors were supported by the Deutsche Forschungsgemeinschaft [Grants HA2800/1-3, HA2800/4-1, GO 766/13-1]; and the Bundesministerium für Bildung und Forschung [Grant UKR 09/004].
K.L. and J.H.H. contributed equally.
Article, publication date, and citation information can be found at http://molpharm.aspetjournals.org.
doi:10.1124/mol.109.057513.

ABBREVIATIONS: TRPC, classic transient receptor potential; DAG, diacylglycerol; DN, dominant negative; PIP_2, phosphatidylinositol-4,5-bisphosphate; TRPV, vanilloid-like transient receptor potential; TRPM, melastatin-like transient receptor potential; TRPN, nompC-like transient receptor potential; NGF, nerve growth factor; YFP, yellow fluorescent protein; PXR, pregnane X receptor; RR, ruthenium red; OAG, 1-oleoyl-2-acetyl-*sn*-glycerol; ACA, *N*-(*p*-amylcinnamoyl)anthranilic acid; HEK, human embryonic kidney; 2-APB, 2-aminophenoxyborate; SK&F 96365, 1-[β-[3-(4-methoxyphenyl)propoxy]-4-methoxyphenethyl]-1*H*-imidazole.

Recent attempts to determine its molecular target led us identify hyperforin as the first and highly selective activator of the TRPC6, a member of the TRP superfamily (Treiber et al., 2005; Leuner et al., 2007).

The TRP superfamily of cation channels encompasses 29 mammalian members. Based on sequence homology and functional data, they can be subdivided in the classic (TRPC), vanilloid-like (TRPV), melastatin-like (TRPM), polycystins, mucolipidin, ankyrine-rich, and nompC-like TRP subfamilies (Montell, 2005, 2006; Voets et al., 2005). TRP channels are homo- and heterotetramers of subunits containing six transmembrane segments (S1–S6) and cytoplasmic N- and C-terminal tails. S5, S6, and the connecting pore loop form the cation-conducting pore. S1–S4 and the cytoplasmic N and C termini are important for channel gating and the interaction with ligands or proteins (Voets et al., 2005; Voets and Nilius, 2007).

TRP channels are involved in a variety of physiological functions. The discovery of their role in temperature sensation and pain was accelerated by the observation that direct and selective activation of TRP channel isoforms underlies the effects of several secondary plant compounds to modulate temperature sensation and cause pain, such as capsaicin, menthol, cinnamaldehyde, gingerol, and camphor (Mandadi and Roufogalis, 2008). TRPC6 is one member of the canonical TRP channel subfamily, which consists of seven members, TRPC1 to TRPC7 (Dietrich and Gudermann, 2007). TRPC channels are highly expressed in the brain and are activated by G-protein-coupled receptors or receptor tyrosine kinases such as mGluR1 or TrkB, which play important roles in neuronal plasticity and memory functions (Jia et al., 2007; Tai et al., 2008; Zhou et al., 2008). The primary mode of activation of TRPC channels in cell physiology is considered to be linked to phospholipase C (Montell, 2005). Phospholipase C-mediated degradation of phosphatidylinositol-4,5-bisphosphate (PIP_2) results in the accumulation of diacylglycerol (DAG), which is considered to be the physiological activator of TRPC3-, TRPC6-, and TRPC7-mediated currents (Hofmann et al., 1999; Trebak et al., 2003; Dietrich and Gudermann, 2007). However, the binding site of DAG at the TRPC6 channel has yet to be identified. Furthermore, several contradicting concepts regarding the activation mechanism of TRPC6 have been discussed. Lemonnier et al. (2008) and Jardín et al. (2008) have reported a significant and pronounced activation of TRPC6 by PIP_2, whereas Kwon et al., (2007) showed a disruption of TRPC6 activity by PIP_2 and propose that PIP_2 metabolites such as phosphatidylinositol (3,4,5)-trisphosphate directly binds to TRPC6 channels and interferes with the calmodulin binding site at the C terminus. The situation became more complex by several reports describing the PIP_2-dependent modulation of TRP channels (Voets and Nilius, 2007). In the case of TRPV1, Brauchi et al. (2007) calculated a homology model with the proposed PIP_2 binding site. From their model, they proposed an interaction of the polar PIP_2 head with a cluster of positively charged amino acids located in the proximal C-terminal region, whereas the aliphatic chains of PIP_2 form hydrophobic interactions with transmembrane domains S5 and S6 of TRPV1 (Brauchi et al., 2007). Overall, different models (direct and indirect) have been described for the interaction of TRPC3/6/7 channels with modulatory acting DAG and PIP_2 (Estacion et al., 2004; Vazquez et al., 2004; Smyth et al., 2006; Nilius et al., 2008).

We recently observed that hyperforin increases TRPC6-mediated nonselective currents. As a nonselective cation channel, TRPC6 is permeable for sodium and for calcium. Thus, it triggers calcium-dependent intracellular signaling processes necessary for cell differentiation (Leuner et al., 2007; Müller et al., 2008). In PC12 cells, hyperforin mimics NGF-induced cellular responses involved in neurite outgrowth (Leuner et al., 2007).

Hyperforin is a polyprenylated bicyclic acylphloroglucinol derivative. Extensive chemical degradation and derivatization studies have established its cage-like structure (Beerhues, 2006). Pure hyperforin is not very stable when exposed to light and oxygen, which limits its clinical applications and further developments. This instability is due to the enolized β-dicarbonyl system present in the molecule. Several previous studies dealt with the chemical modification of its structure by acylation, alkylation, and oxidation but not with a chemical simplification of hyperforin to identify new stable and potent hyperforin analogs (Tada et al., 1992; Verotta et al., 1999, 2000, 2004). It is noteworthy that the core structure of hyperforin, the phloroglucinol, is rather stable. Based on the perspective of potential therapeutic applications, we became interested in the search for stable synthetic phloroglucinol derivatives with pharmacological activity profiles comparable with that of hyperforin and acting as TRPC6-selective agonists.

As a consequence, we selected simple 2-acylphloroglucinol and 2,4-diacylphloroglucinol derivatives and tested them for their hyperforin-like bioactivities. Selection of nine compounds from phloroglucinol derivatives reported in the literature (Tada et al., 1992) was conducted on the basis of our working hypothesis that the phloroglucinol moiety provides the essential pharmacophore of hyperforin and that its activity profile could be due to structural resemblances to DAG, PIP_2, and some polyunsaturated-free fatty acids (Fig. 1). A variety of methods were selected to cover all functional aspects of TRPC6 activation from single-channel activity, Ca^{2+} imaging, and functional aspects such as neurite outgrowth and inhibition of synaptosomal uptake.

Materials and Methods

Sources and Preparation of Reagents. Hyperforin and all phloroglucinol derivatives tested were kindly supplied by the preclinical Research Department of Dr. Willmar Schwabe (Karlsruhe, Germany).

1-Oleoyl-2-acetyl-*sn*-glycerol (OAG; Sigma-Aldrich, Taufkirchen, Germany) and phloroglucinol was used from 100 mM stock solution in dimethyl sulfoxide. NGF (Sigma-Aldrich) was dissolved in distilled water and prepared in 50 μg/ml stock solution. $GdCl_3$ and $LaCl_3$ (Sigma-Aldrich) were dissolved in H_2O before experiments. Other chemicals were dissolved in dimethyl sulfoxide in stock solutions and diluted before use. For pharmacological treatments, chemicals were present throughout the experiment.

[^{3}H]Serotonin was obtained from BIOTREND Chemicals GmbH (Cologne, Germany), and Lumasafe scintillation cocktail was from PerkinElmer Life and Analytical Sciences (Waltham, MA). Standard laboratory chemicals were obtained from Sigma-Aldrich. The nine 2-acyl- and 2,4-diacylphloroglucinol derivatives used in this study (Hyp1–9) were synthesized, purified, and characterized according to the methods of Tada et al. (1992).

Cell Culture and Transfection of HEK293 Cells and PC12 Cells. HEK293 cells were cultured in Dulbecco's modified Eagle's

medium (Invitrogen, Groningen, The Netherlands) with 10% heat-inactivated fetal calf serum (Sigma-Aldrich), 50 U/ml penicillin (Sigma-Aldrich), and 50 μg/ml streptomycin (Sigma-Aldrich) at 37°C under a 5% CO_2 humidified atmosphere at 37°C. Cells were plated in 85-mm dishes onto glass coverslips and were transiently transfected 24 h later by the addition of a transfection cocktail containing 0.5 to 1 μg of DNA and 1 to 2 μl of FuGENE 6 transfection reagent (Roche Diagnostics, Indianapolis, IN) in 97 μl of Opti-MEM medium (Invitrogen). The cDNA constructs for TRPC3, TRPC6, and TRPC7 were kindly provided by Dr. Michael Schaefer. Fluorescence measurements and electrophysiological studies were carried out 1 to 2 days after transfection. PC12 cells were cultured in Dulbecco's modified Eagle's medium supplemented with 10% heat-inactivated fetal calf serum and 5% heat-inactivated horse serum, 50 U/ml penicillin, and 50 μg/ml streptomycin at 37°C in a humidified incubator containing 5% CO_2. Before Ca^{2+} imaging, cells were plated in 85-mm dishes onto glass coverslips. Transient transfection of PC12 cells was conducted using FuGENE 6 transfection reagent (Roche Diagnostics). Cells were plated in 85-mm dishes onto glass coverslips and were transiently transfected by the addition of a transfection cocktail containing 0.5 to 1 μg of DNA and 2 μl of FuGENE 6 transfection reagent (Roche Diagnostics) in 97 μl of Opti-MEM medium (Invitrogen). Fluorescence measurements were conducted 2 days after transfection. Neurite outgrowth assays were conducted 3 days after transfection.

Patch-Clamp Experiments. Membrane currents were recorded using the perforated whole-cell configuration of the patch-clamp technique at room temperature. Pipettes were made from borosilicate glass capillary tubes. The pipette resistance was 4 to 5 MΩ. Currents through the pipette were recorded by an Axopatch 200B amplifier (Molecular Devices, Sunnyvale, CA), filtered at 2 kHz (Bessel filter) and digitized at 5 kHz. Data acquisition and command potentials were controlled with commercial software programs using a CED1401 interface (Cambridge Electronic Design Limited, Cambridge, UK) or Iso2 (MFK, Taunusstein, Germany). Whole-cell currents were elicited by voltage ramps from −100 to +100 mV (400 ms duration) applied every 10 s from a holding potential of −40 mV. The standard bath solution contained 140 mM NaCl, 5 mM KCl, 2 mM $CaCl_2$, 1 mM $MgCl_2$, 10 mM glucose, and 10 mM HEPES, pH 7.4, with NaOH. Pipettes were filled with a solution containing amphotericin B (250 mg/ml) in 100 mM cesium-aspartate, 40 mM CsCl, 0.4 mM $CaCl_2$, 2 mM $MgCl_2$, 1 mM EGTA, and 10 mM HEPES, pH 7.2, with CsOH. Analyzed data were expressed as mean ± S.E.M., and a paired Student's t test was used for data comparison with the level of significance set at $P < 0.05$.

Fluorescence Measurements. $[Ca^{2+}]_i$ measurements in single cells were carried out using the fluorescence indicator Fura-2/acetoxymethyl ester in combination with a monochromator-based imaging system (TILL Photonics, Martinsried, Germany; or Attofluor Ratio Vision system, Atto Instruments, Rockville, MD) attached to an inverted microscope (Axiovert 100; Carl Zeiss, Oberkochen, Germany). HEK293 cells and PC12 cells were loaded with 4 μM Fura-2/acetoxymethyl ester and 0.01% Pluronic F-127 (both from Invitrogen) for 45 min at room temperature in a standard solution composed of 138 mM NaCl, 6 mM KCl, 1 mM $MgCl_2$, 2 mM $CaCl_2$, 5.5 mM glucose, and 10 mM HEPES adjusted to pH 7.4 with NaOH. Coverslips were then washed in this buffer for 20 min and mounted in a perfusion chamber on the microscope stage. For $[Ca^{2+}]_i$ measurements, fluorescence was excited at 340 and 380 nm. After correction for background fluorescence, the fluorescence ratio F_{340}/F_{380} was

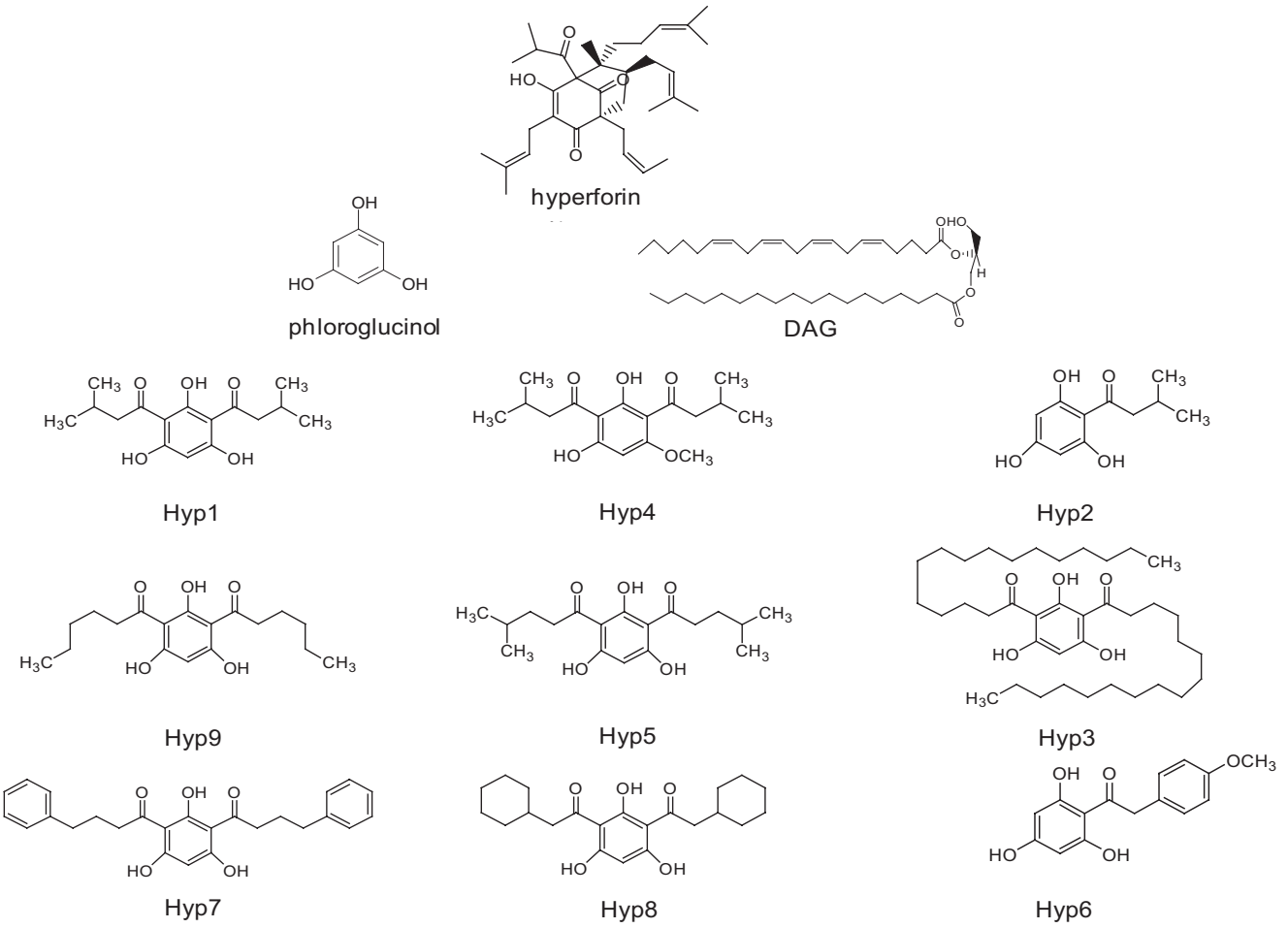

Fig. 1. Structures of hyperforin, DAG, PIP_2, phloroglucinol, and the phloroglucinol derivatives tested.

calculated. For $[Ba^{2+}]_i$ and $[Sr^{2+}]_i$, cells were washed three times after incubation with Ca^{2+}-free standard solution. The influx of Ba^{2+} and Sr^{2+} was evaluated in Fura-2-loaded cells by measuring the fluorescence of Ba^{2+} or Sr^{2+} Fura complexes.

Synaptosomal Serotonin Uptake. For neurotransmitter uptake experiments, synaptosomal preparations were obtained from whole brain of 2- to 3-month-old female mice. The tissue was homogenized in ice-cold sucrose solution (0.32 M) and diluted with 10 ml of the homogenizing medium. The nuclear fraction was eliminated by centrifugation at 750*g* for 10 min (Beckman centrifuge; Beckman Coulter, Fullerton, CA). The supernatant was centrifuged at 17,400*g* for 20 min to obtain the crude synaptosomal pellets. The pellets were suspended in 11 ml of ice-cold Krebs-HEPES buffer (150 mM NaCl, 10 mM HEPES, 6.2 mM KCl, 1.2 mM Na_2HPO_4, 1.2 mM $MgSO_4$, 10 mM glucose, 10 mM pargyline, and 0.1% ascorbic acid, pH 7.4, at 37°C), aliquoted in microtiter plates, incubated in the presence of varying concentrations of the drugs tested at 37°C for 15 min in a shaking water bath, and cooled on ice. [^{3}H]Serotonin (2.9 nM) was added, and the uptake experiment was started by incubation at 37°C for 4 min. The probes were cooled, immediately filtered through Whatman GF/B glass fiber filters (Whatman, Clifton, NJ), and washed three times with ice-cold buffer solution with a Brandel cell harvester (Brandel Inc., Gaithersburg, MD). Filters were placed in plastic scintillation vials containing 4 ml of Lumasafe scintillation cocktail (PerkinElmer Life and Analytical Sciences). Radioactivity was measured after 12 h. Nonspecific uptake was determined in parallel probes maintained throughout on ice or containing unlabeled serotonin (1 mM serotonin).

Neurite Outgrowth of PC12 Cells. Cells were plated at a density of nine cells per plate (85 mm, polylysine-coated) in 15% serum-containing medium overnight. The next day, medium was changed to a medium containing 2% serum and NGF (50 ng/ml), hyperforin, the 2,4-diacylphloroglucinols, or hyperforin and 2,4-diacylphloroglucinols supplemented with La^{3+} or Gd^{3+}. The neurite length was examined 3 days after different treatment regimens. After 3 days, PC12 cells were fixed with paraformaldehyde solution (4%) and stained with Mayer's hematoxylin and eosin solutions. Thereafter, 10 cells from each stain (n = 1) were arbitrarily investigated, and neurite length was detected by using Nikon NIS Elements AR 2.1 software (Nikon, Tokyo, Japan).

Pharmacophore Alignment. Based on the crystal structure of hyperforin in complex with the pregnane X receptor [Protein Data Bank identifier 1m13 (Watkins et al., 2003), resolution 2.15 Å] all atoms involved in hydrogen bridges were classified as hydrogen bond donors or acceptors, and the core was classified as hydrophobic. Three of four hydrogen bonds were regarded as essential (interaction with Ser247, His407, and Gln285), and the fourth bond to a water molecule was considered optional, because water molecules cannot be expected at similar positions in TRPC6. Flexible pharmacophore-based alignments were performed with the software MOE (version 2008.9; Chemical Computing Group, Montreal, QC, Canada). The minimal number of matched features was set to three. For the depiction of results, we used Pymol version 1.0 (available at http://www.pymol.org).

Results

Inhibition of Serotonin Uptake. Several phloroglucinol derivatives were selected to investigate our working hypothesis that the phloroglucinol moiety of hyperforin represents its essential pharmacophore and that its structural resemblance to DAG, PIP_2, and polyunsaturated fatty acids might explain its observed activity profile. We first tested the effects of phloroglucinol, DAG, and several 2-acyl- and 2,4-diacylphloroglucinols on serotonin uptake (Fig. 1). Thereafter, we determined the IC_{50} values of the selected substances in comparative experiments with hyperforin. The [^{3}H]seroto-

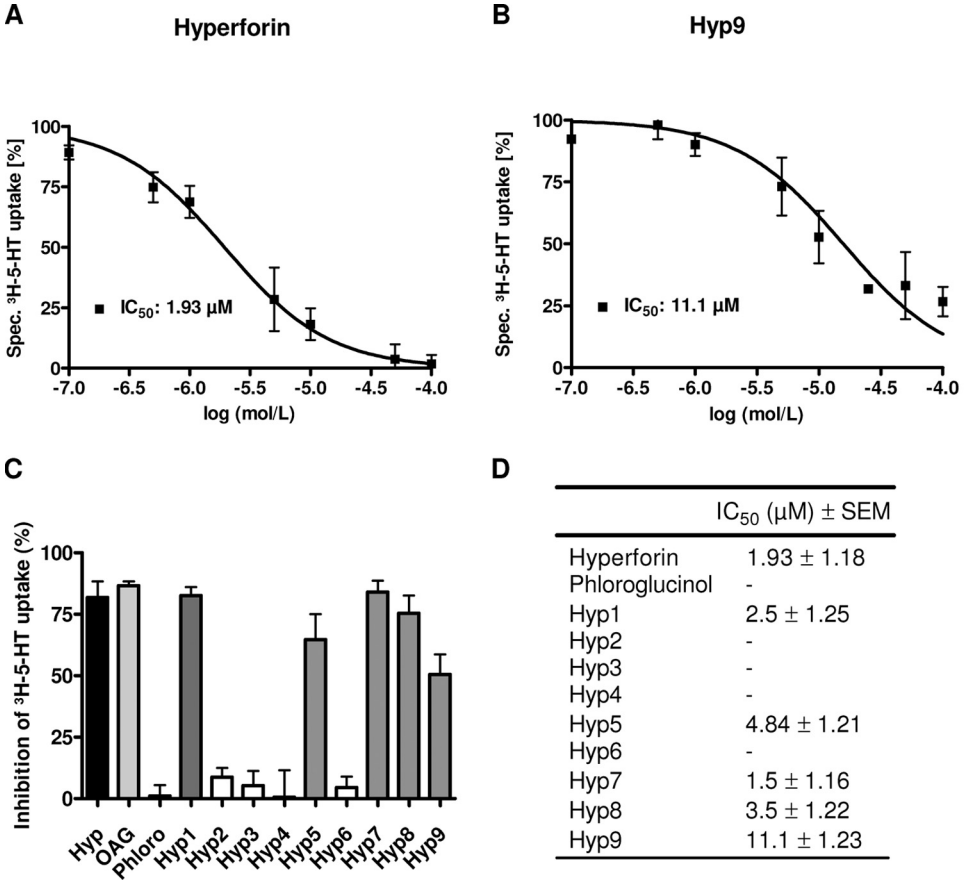

	IC_{50} (µM) ± SEM
Hyperforin	1.93 ± 1.18
Phloroglucinol	-
Hyp1	2.5 ± 1.25
Hyp2	-
Hyp3	-
Hyp4	-
Hyp5	4.84 ± 1.21
Hyp6	-
Hyp7	1.5 ± 1.16
Hyp8	3.5 ± 1.22
Hyp9	11.1 ± 1.23

Fig. 2. Effects of hyperforin, phloroglucinol, and its derivatives on serotonin uptake in murine synaptosomes. Serotonin uptake was measured using [^{3}H]serotonin in murine synaptosomes. The synaptosomes were preincubated for 15 min with varying concentrations of hyperforin, phloroglucinol, and its derivatives. Concentration-response curves are shown for the inhibition of [^{3}H]serotonin uptake by hyperforin (A) and by Hyp9 (B). C, summary of the effects of the hyperforin, phloroglucinol, and the different hyperforin derivatives at a concentration of 10 μM on serotonin uptake. D, IC_{50} values obtained for the phloroglucinol derivatives and phloroglucinol are compared with the IC_{50} of hyperforin (error bars indicate ±S.E.M., n = 6).

nin uptake in murine synaptosomes was inhibited by hyperforin with an IC_{50} value of 1.93 μM (Fig. 2A), whereas the uptake was blocked by Hyp9 with an IC_{50} value of 11.1 μM (Fig. 2B). To further analyze the functional capability of the selected derivatives, we compared the inhibitory effect at a single concentration (10 μM) (Fig. 2C). Like hyperforin, and the endogenous activator of TRPC6 OAG (100 μM), Hyp1, Hyp5, Hyp7, Hyp8, and Hyp9 inhibited serotonin uptake in murine synaptosomes with comparable IC_{50} values ranging from 1.5 μM for Hyp7 to 11.1 μM for Hyp9 (Fig. 2D). Phloroglucinol, Hyp2, Hyp3, Hyp4, and Hyp6 failed to inhibit serotonin uptake. These data clearly suggest that 2,4-diacylphloroglucinol structures can mimic hyperforin-mediated effects and that they could represent a novel class of easily accessible pharmacophores.

2,4-Diacylphloroglucinols Induce Neurite Outgrowth. TRPC6 channels are highly expressed in the brain and are involved in local processes such as growth-cone turning, neurite extension, the formation of excitatory synapses, and spatial learning and memory (Li et al., 2005; Tai et al., 2008). We have shown previously that hyperforin is able to induce neurite outgrowth in PC12 cells at clinically relevant concentrations of 0.3 μM (Leuner et al., 2007). Therefore, we investigated the effects of phloroglucinol and all phloroglucinol derivatives on neurite outgrowth. PC12 cells were incubated for 3 days with 0.3 μM phloroglucinol, hyperforin, the derivatives, or 50 ng/μl NGF. Differentiation of PC12 cells was determined by measuring neurite lengths in PC12 cells after 3 consecutive days of treatment. Hyp1, Hyp5, Hyp7, Hyp8, and Hyp9 induced neurite outgrowth comparable with the effect induced by hyperforin or NGF (Fig. 3, A and B). Phloroglucinol and Hyp2, Hyp3, Hyp4, and Hyp6 were ineffective.

Because we showed previously that the induction of neurite outgrowth is mediated by TRPC6 channels, we next tested the role of these channels to further characterize the pharmacological profile of the new structures. We used pharmacological and genetic approaches to interfere with TRPC6 activity. First, PC12 cells were incubated with the TRP channel blockers lanthanum (100 μM) and gadolinium (100 μM) ions in the presence of the active phloroglucinol derivatives. The neurite outgrowth induced by Hyp1, Hyp5, Hyp7, Hyp8, and Hyp9 was dramatically reduced by the coincubation with gadolinium and lanthanum (Fig. 3C). These results are consistent with TRPC6-mediated effects. This presumption was

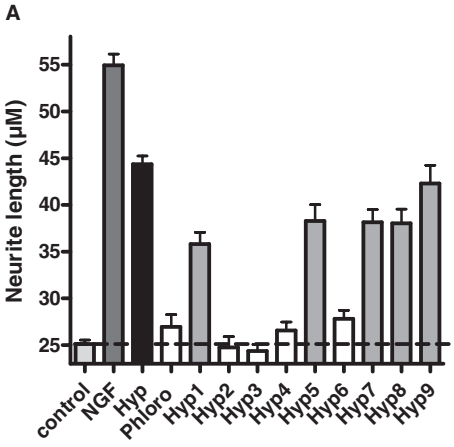

C

	% Inhibition	
	+La^{3+}	+Gd^{3+}
Hyp	62	64
Hyp1	68	70
Hyp5	63	65
Hyp7	65	68
Hyp8	66	70
Hyp9	59	60

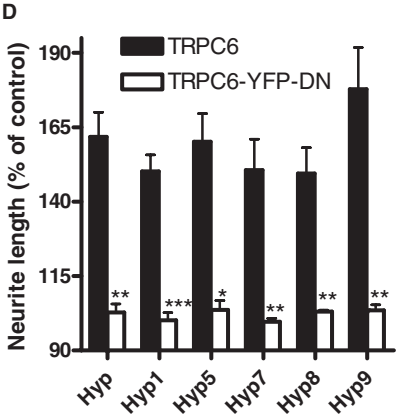

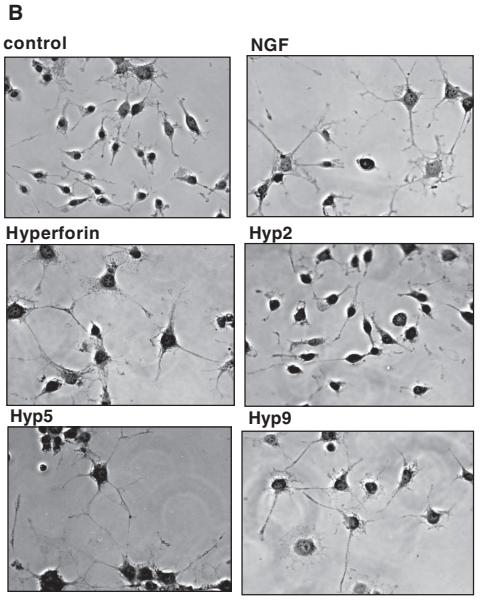

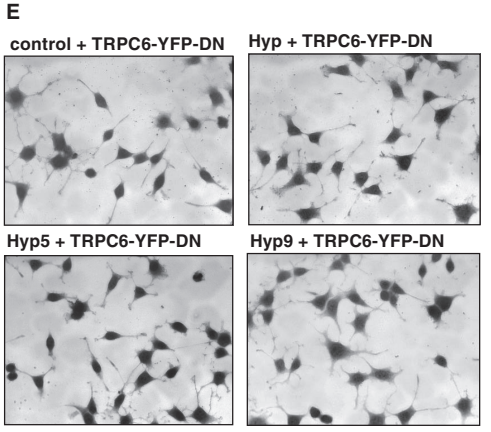

Fig. 3. Phloroglucinol derivatives induce neurite outgrowth in PC12 cells via TRPC6 activation. Neurite outgrowth assays were performed using PC12 cells. A, PC12 cells were treated with NGF (50 ng/ml), hyperforin, phloroglucinol, and hyperforin derivatives (0.3 μM) for 3 consecutive days. After a 3-day incubation period, the average neurite extension was measured, and the data of treated cells were compared with NGF-stimulated PC12 cells. Hyp1, Hyp5, Hyp7, Hyp8, and Hyp9 induced a significant neurite outgrowth (error bars indicate ±S.E.M.; $n = 6$; unpaired t test, $P < 0.01$). B, representative images of PC12 cells with neurite extensions are shown from experiments after a 3-day incubation period in untreated control cells and in cells in the presence of NGF (50 ng/ml), hyperforin (0.3 μM), Hyp2 (0.3 μM), Hyp5 (0.3 μM), and Hyp9 (0.3 μM) ($n = 6$). C, Neurite extension induced by hyperforin or the active phloroglucinol derivatives was measured in the presence and absence of La^{3+} (100 μM) or Gd^{3+} (100 μM) for 5 days. Results are expressed as the percentage of the neurite length average in the absence of the TRP channel blockers. Both inhibitors blocked the effect of Hyp1, Hyp5, Hyp7, Hyp8, and Hyp9 significantly (error bars indicate ± S.E.M.; $n = 6$; unpaired t test, $P < 0.001$). D, TRPC6-DN-YFP-expressing and untransfected PC12 cells were treated with hyperforin (0.3 μM) and the active phloroglucinol derivatives 24 h after transfection and differentiated over 3 consecutive days. Representative images were taken, and neurite lengths were measured. The data given in the bars compare neurite outgrowth in TRPC6-DN-YFP-expressing and untransfected PC12 cells under the treatment with hyperforin and the respective derivatives. E, representative images of PC12 cells expressing TRPC6-DN-YFP treated with hyperforin (0.3 μM), Hyp5 (0.3 μM), or Hyp9 (0.3 μM) ($n = 3$, error bars indicate S.E.M., unpaired t test, *, $P < 0.05$, **, $P < 0.01$, ***, $P < 0.001$).

further validated by a genetic approach using a dominant-negative TRPC6 mutant. We transiently transfected PC12 cells with TRPC6-DN-YFP and incubated the transfected cells for 2 days in the presence of the active phloroglucinol derivatives. In TRPC6-DN-YFP-expressing cells, the Hyp1-, Hyp5-, Hyp7-, Hyp8-, and Hyp9-induced outgrowth of neurites was completely abolished, which strongly argues for the involvement of TRPC6 channels in the 2,4-diacylphloroglucinol-induced neurite outgrowth.

Symmetric 2,4-Diacylphloroglucinols Induce Nonselective Cation Influx in PC12 Cells. To provide further evidence that 2,4-diaclyphloroglucinol represents the active core of hyperforin pharmacophore, we studied Ca^{2+} and Ba^{2+} fluxes by imaging techniques using the intracellular calcium indicator Fura-2. The experimental set-up was comparable with the approaches described before. Hyperforin and the phloroglucinol structures were applied at concentrations of 10 μM to Fura-2-loaded PC12 cells. Hyp1, Hyp5, Hyp7, Hyp8, and Hyp9 induced a robust and transient elevation of $[Ca^{2+}]_i$, which is comparable with that of hyperforin (Fig. 4, A and C). Hyp2, Hyp3, Hyp4, and Hyp6 failed to increase $[Ca^{2+}]_i$ (Fig. 4, B and C). EC_{50} values determined for the active compounds were comparable with that of hyperforin and ranged from 1.26 μM for Hyp9 to 7.17 μM for Hyp8. In

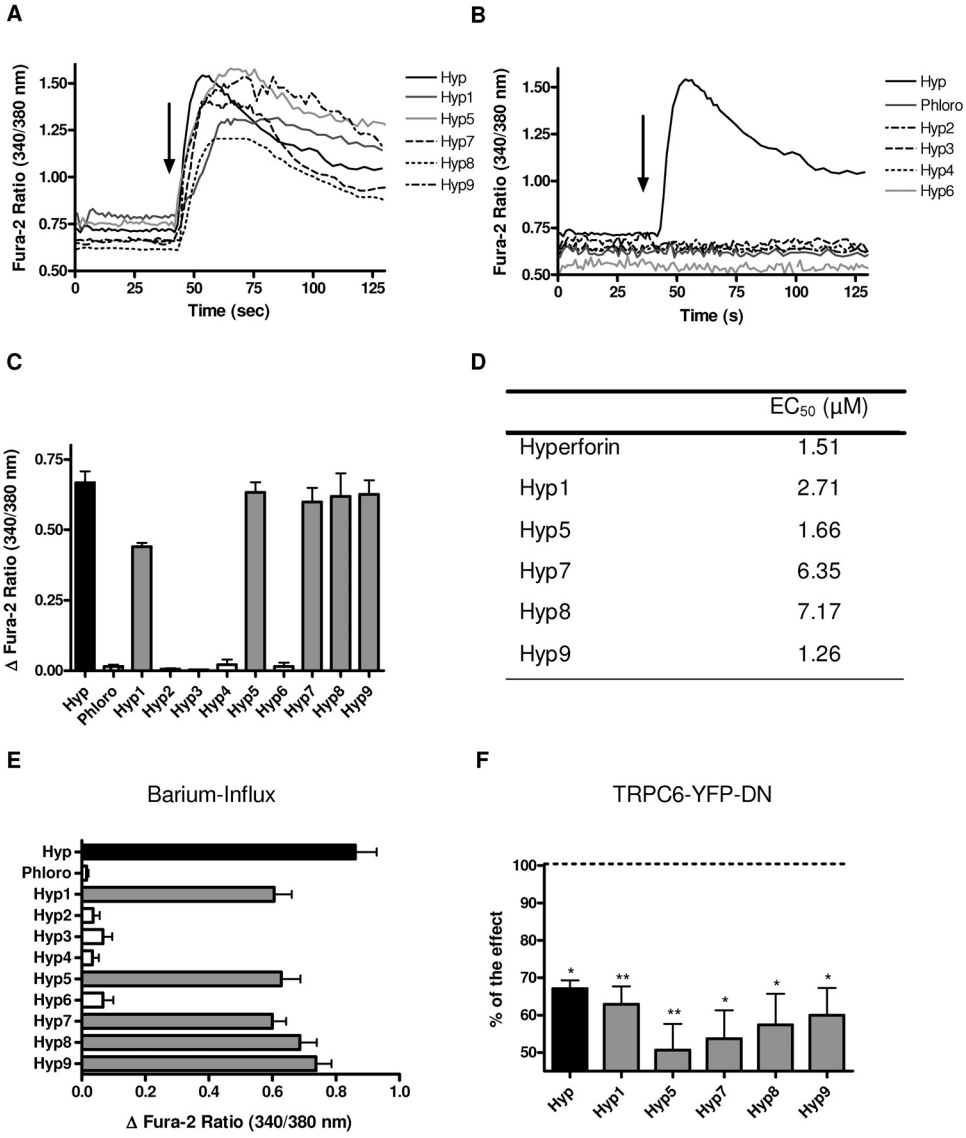

	EC_{50} (μM)
Hyperforin	1.51
Hyp1	2.71
Hyp5	1.66
Hyp7	6.35
Hyp8	7.17
Hyp9	1.26

G

	% Inhibition of Ca^{2+}-Influx					
	+ La^{3+} (100 μM)	+ Gd^{3+} (100 μM)	+ SK&F (10 μM)	+ RR (1 μM)	+ ACA (30 μM)	+ 2-APB (30 μM)
Hyperforin	64	74	80	ns	35	63
Hyp1	51	65	61	ns	55	47
Hyp5	64	64	64	ns	37	48
Hyp7	62	68	62	ns	46	63
Hyp8	55	63	48	ns	54	71
Hyp9	57	64	62	ns	35	41

Fig. 4. Phloroglucinol derivatives induce a nonselective cation influx in PC12 cells via TRPC6. Hyperforin and phloroglucinol derivative-induced changes in $[Ca^{2+}]_i$ were characterized in Fura-2-loaded PC12 cells in video-imaging experiments as described under *Materials and Methods*. A, representative time traces show hyperforin and Hyp1-, Hyp5-, Hyp7-, Hyp8-, and Hyp9-induced elevation of $[Ca^{2+}]_i$ (10 μM; $n = 6$). B, representative traces from experiments using hyperforin, phloroglucinol, Hyp2, Hyp3, Hyp4, and Hyp 6 are given (10 μM; $n = 6$). C, summarized effects of hyperforin, phloroglucinol, and the phloroglucinol derivatives (10 μM) on intracellular Ca^{2+} concentrations in PC12 cells. D, EC_{50} values for hyperforin and the active derivatives Hyp1, Hyp5, Hyp7, Hyp8, and Hyp9 were calculated from Ca^{2+} imaging experiments. E, nonselective cation influx induced by hyperforin, phloroglucinol, and the different hyperforin derivatives was measured replacing $[Ca^{2+}]_{ex}$ by 2 mM Ba^{2+} using Fura-2 fluorescence. To identify the molecular structure of the hyperforin derivative-activated entry mechanism, we used a dominant-negative knockdown of TRPC6 that was tagged with YFP (TRPC6-DN-YFP) (F) and different TRP channel blockers (G). F, Fura-2-loaded, TRPC6-DN-YFP-expressing PC12 cells were stimulated with hyperforin and the active derivatives and were compared with untransfected cells (errors bars indicate ±S.E.M., $n = 6$, 5–10 cells per independent experiment; unpaired t test, *, $P < 0.05$, **, $P < 0.01$, ***, $P < 0.001$). The results are expressed as a percentage of effect of the respective untransfected control treated with the different stimuli. G, summary of changes in $[Ca^{2+}]_i$ in percentage induced by hyperforin and the respective derivatives in the presence of SK&F 96365 (10 μM, $n = 6$), La^{3+} (100 μM, $n = 6$), Gd^{3+} (100 μM, $n = 6$), 2-APB (30 μM, $n = 6$), ACA (30 μM, $n = 6$), and RR (1 μM) normalized on the Ca^{2+} influx in the absence of the different blockers are shown in G. SK&F 96365, La^{3+}, and Gd^{3+} significantly inhibited the Ca^{2+} influx induced by hyperforin and the different derivatives with P values smaller than 0.001; ACA and 2-APB with P values between 0.05 and 0.01, respectively. RR showed no effect on Ca^{2+} influx (ns, not significant). Error bars indicate ±S.E.M., unpaired t test.

addition, the measurements of Ba^{2+} entry showed a comparable profile of the test compounds (Fig. 4E). Transfection of PC12 cells with the dominant-negative TRPC6 construct before Fura-2 loading of the cells diminished the stimulatory effect of the 2,4-diacylphloroglucinols (Fig. 4F). To finally complete the pharmacological profile of the 2,4-diaclyphloroglucinols, we used gadolinium (100 μM) and lanthanum ions (100 μM), SK&F 96365 (10 μM), *N*-(*p*-amylcinnamoyl)anthranilic acid (ACA; 30 μM), and 2-aminophenoxyborate (2-APB; 30 μM) known to interfere with nonselective cation channels, especially TRPC channels (Fig. 4G). Because the profile of the compounds strongly argued for the involvement of TRP channels in the derivative-induced Ca^{2+} influx, we also tested ruthenium red (RR) (10 μM), which blocks TRPV, TRPM6, TRPM8, and ankyrine-rich transient receptor potential-1 channels (Leuner et al., 2007). RR had no effect on hyperforin-induced calcium entry and thereby allowed us to narrow down the variety of putative candidates mainly to TRPC channels. The results are summarized in Fig. 4G and are consistent with the idea that 2,4-diacylphloroglucinols represent the pharmacophore of hyperforin.

TRPC6-Mediated Currents Are Induced by 2,4-(1-Ketohexyl) Phloroglucinol (Hyp9). Based on the EC_{50} values determined for the active 2,4-diacylphoroglucinol derivatives (Fig. 4D), we chose the most potent structure for electrophysiological characterization in whole-cell patch-clamp experiments. As shown in Fig. 5, Hyp9 (10 μM) markedly stimulated whole-cell currents in TRPC6-expressing HEK293 cells (Fig. 5, A and B). Mean current densities at +90 and −90 mV measured after 3 to 5 min of application of Hyp9 were significantly increased in TRPC6-transfected cells (Fig. 5B). The current increase was blocked by subsequent application of Gd^{3+} (100 μM). Thus, these effects were similar compared with the effects of hyperforin on recombinant TRPC6 channels in HEK293 cells (Leuner et al., 2007).

In addition to recombinantly expressed TRPC6 channels in HEK293 cells, we studied the activation of natively expressed TRPC6-like channels by hyperforin and Hyp9 in PC12 cells, the cell model also used for experiments testing the capability of hyperforin and the Hyp derivatives to enhance neurite outgrowth. Whole-cell patch-clamp experiments were performed in the absence (Fig. 5, C and D) and presence of gadolinium ions (100 μM) (Fig. 5, E and F). Hyperforin (10 μM, Fig. 5C) and Hyp9 (10 μM, Fig. 5D) induced similar inward and outward currents over time. Upon application, currents developed over time with maxi-

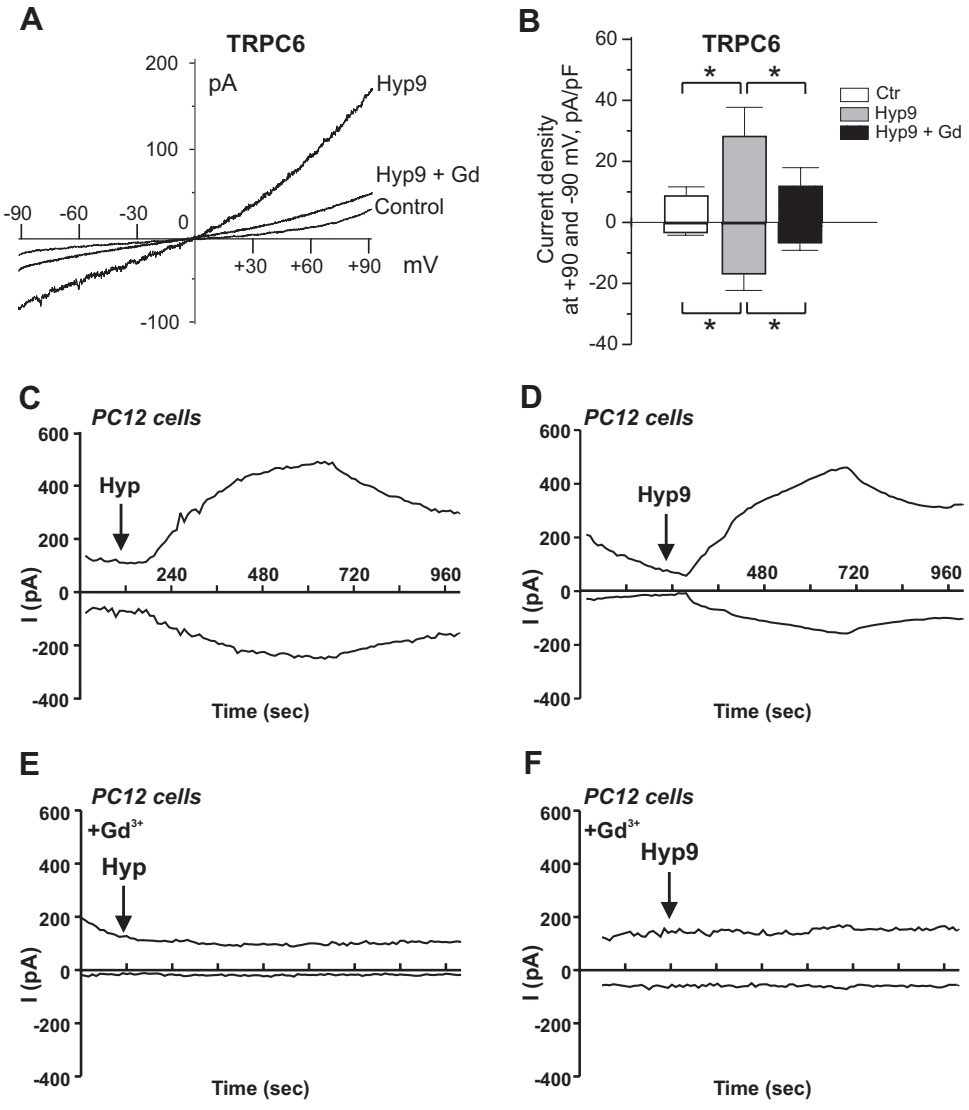

Fig. 5. Phloroglucinol derivatives induced TRPC6 currents. Application of Hyp9 (10 μM) resulted in the significant increase in outward and inward currents in TRPC6-expressing HEK293 cells and PC12 cells. A, whole-cell currents elicited by voltage ramps from −100 to +100 mV in TRPC6-expressing HEK293 cell from a holding potential of −40 mV in control (Control) after application of 10 μM Hyp9 (Hyp9) and 10 μM Hyp9 plus 100 μM Gd^{3+} (Hyp9 + Gd). B, mean current density at + 90 and −90 mV in control (□) and after 3- to 5-min application of 10 μM Hyp9 (▨) and 10 μM Hyp9 plus 100 μM Gd^{3+} (■) in TRPC6-expressing cells (n = 7) (*, $P < 0.05$). C to F, in the absence (C and D) and presence (E and F) of Gd^{3+} (100 μM), whole-cell currents were recorded from PC12 cells stimulated by hyperforin (C and E) and Hyp9 (D and F). The currents measured at + 90 and −90 mV are plotted over time. Shown are representative experiments (n = 4 in each group); the time scale is similar in each.

mal current amplitudes after 5 min. In the presence of Gd^{3+} (100 μM), neither hyperforin- nor Hyp9-induced currents were detectable (Fig. 5, E and F). The current-voltage relationships of both hyperforin- and Hyp9-induced currents in PC12 cells elicited by voltage ramps were almost linear and comparable with values shown for currents recorded from recombinantly expressed TRPC6.

2,4-Diacylphloroglucinols Selectively Activate TRPC6. Diacylglycerol activates TRPC3, TRPC6, and TRPC7, whereas hyperforin selectively stimulates only TRPC6. We next studied the central question of whether the pronounced TRPC6 selectivity of 2,4-diacylphloroglucinol derivatives has been conserved or lost by these compounds. Therefore, we transiently expressed TRPC3, TRPC6, and TRPC7 protein as YFP fusion proteins in HEK293 cells (Fig. 6). The functional expression was verified by the application of OAG (100 μM) before the addition of hyperforin (10 μM) (Fig. 6A) and Hyp5 (Fig. 6B). In both experimental configurations, the substances induced transient effects in TRPC6-expressing cells, whereas the fluorescence remained unchanged in TRPC3- and TRPC7-expressing cells. The statistical analysis of these experiments is given in Fig. 6, C to E. The data show that the 2,4-diacylphloroglucinol derivative carry not only the active moiety of hyperforin but also the selectivity to TRPC6. Based on the different experimental data, we started with structure-activity relationship evaluations to determine whether a binding site for the known stimulating drugs can be extracted.

Predicted Ligand Binding Modes for Hyperforin, DAG, and the Phloroglucinol Derivatives. Because an experimentally determined three-dimensional structure of the DAG or hyperforin binding pocket in TRPC6 is unavailable, we analyzed the hyperforin derivatives and DAG regarding their possible binding conformation using the complex of pregnane X receptor and hyperforin as a reference (Watkins et al., 2003). Because PXR binds hyperforin in a supposedly bioactive form, we used this complex to define potential pharmacophoric points for the interaction with TRPC6. The bound hyperforin conformation provided detailed information about essential interaction points and was adapted for the prediction and evaluation of hyperforin and phloroglucinol derivatives and their substructural features.

By applying modeling techniques (Jones et al., 1995; Lovell et al., 2003) for automated molecular docking, we could define a common binding mode for hyperforin and DAG, the putative endogenous ligand. We selected three amino acids as essential for binding from the receptor site of PXR and designed a procedure to test the hypothesis that hyperforin derivatives show similar interactions, which might also be present in TRPC6. We focused on Hyp2 and on Hyp7. Prediction of possible binding modes for TRPC6 binding ligands was performed with two modeling approaches, including molecular docking and pharmacophore alignment.

At first, DAG was docked into the PXR receptor so that three oxygens could be predicted to interact with residues in a man-

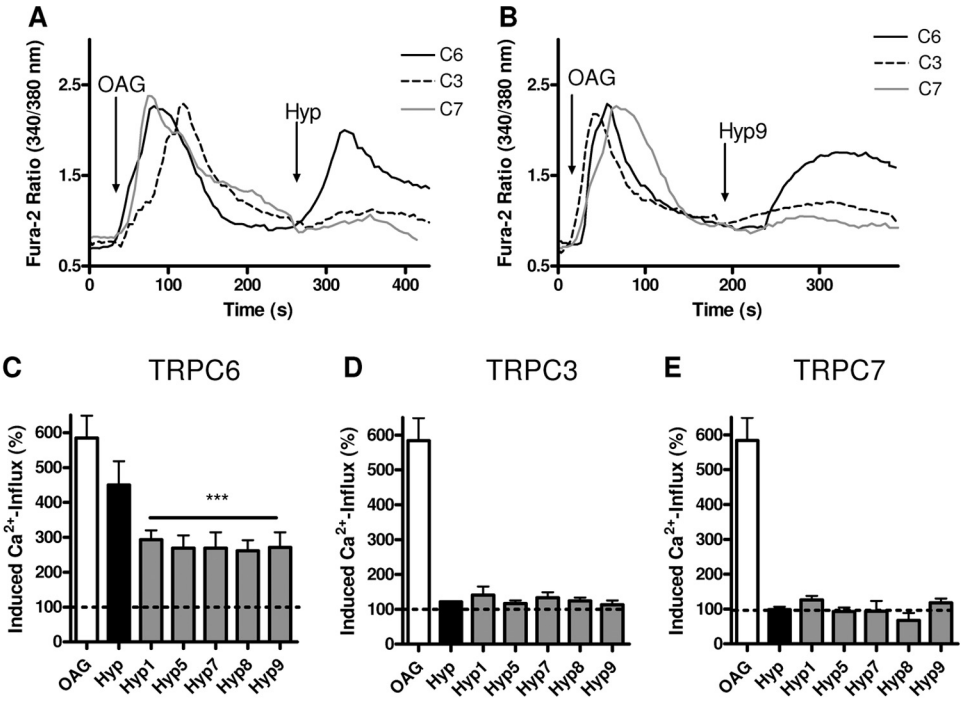

Fig. 6. Phloroglucinol derivatives activate TRPC6 channels. To determine whether the active hyperforin derivatives are selective TRPC6 activators or also are activate closely related TRPC3 or TRPC7 channels, we studied the effects of the derivatives in TRPC3-, TRPC6-, and TRPC7-expressing HEK293 cells in single-cell measurements. TRPC proteins were transiently expressed as C-terminal YFP fusion proteins in HEK293 cells. Functional expression of the proteins was monitored by the application of either OAG (100 μM) before the application of hyperforin or the respective derivative (10 μM). A and B, single traces of changes in fluorescence were monitored from TRPC6-YFP- (red), TRPC3-YFP- (black), or TRPC7-YFP-expressing HEK293 cells stimulated with hyperforin (A) or Hyp9 (B). Cells were consecutively stimulated with OAG (100 μM), hyperforin (10 μM; $n = 6$), or Hyp9 (10 μM). Hyperforin and Hyp9 only induced a significant Ca^{2+} increase in TRPC6-YFP-expressing HEK293. Only OAG induced changes in fluorescence in TRPC3-YFP-, TRPC6-YFP, and TRPC7-YFP-expressing cells. C, D, and E, summary of experiments of TRPC6-YFP-, TRPC3-YFP-, and TRPC7-YFP-expressing HEK293 cells treated with hyperforin and all active phloroglucinol derivatives (10 μM). Exclusively in TRPC6-expressing HEK293 cells, hyperforin and Hyp1, Hyp5, Hyp7, Hyp8, and Hyp9 induced a significantly increased Ca^{2+} influx. Ca^{2+} elevation is expressed as a percentage compared with untransfected HEK293 cells (error bars indicate ±S.E.M., $n = 3$; unpaired t test, ***, $p < 0.001$).

ner similar to that of hyperforin (Fig. 7). The docking procedure constrained the hydrogen bonds to the same protein protonation state as observed for hyperforin and PXR. However, docking of synthesized phloroglucinol derivatives did not allow for the discrimination between the "up" and "down" orientation of the ligand in the binding pocket (Fig. 8B) but suggests an interaction with identical side chains regardless of the ligand orientation. Thus, pharmacophore alignment was applied, and the result was in agreement with the "down" conformation of the ligand (Fig. 8A). The "down" conformation is in better agreement with experimental findings, which suggest that both carbonyl groups of the derivates are essential for activity: ligand derivatives lacking a second carbonyl function were inactive in activity assays (e.g., Hyp3).

Discussion

Starting with the challenging job of the development of stable phloroglucinol derivatives carrying the pharmacological properties of hyperforin, we finally identified five 2,4-diacylphloroglucinol derivatives meeting the initial demand. By extensive pharmacological characterization, including transmitter uptake, neurite outgrowth, calcium imaging assays, electrophysiological recordings, and modeling approaches, we identified symmetric 2,4-diacylphloroglucinol derivatives as potent and selective hyperforin-like TRPC6 activators.

We tested our working hypothesis that the phloroglucinol moiety of hyperforin represents the essential pharmacophore and reflects a structural resemblance to DAG, PIP_2, and polyunsaturated fatty acids might be important for activity. It is noteworthy that phloroglucinol itself failed to inhibit serotonin uptake and activate TRPC6 channels. Only the symmetric 2,4-diacylphloroglucinol derivatives, which possess acyl chains composed of one to five carbons or acyl chains composed of one to two carbons substituted with a benzene ring, led to a pronounced activation of TRPC6 channels. To our surprise, long aliphatic side chains observed in Hyp3 with 15 carbons did not activate TRPC6 channels. In addition, nonsymmetric 2-acylphloroglucinol derivatives such as Hyp2 or Hyp6 showed no effect on TRPC6 channels. Methylation of one of the hydroxyl functions of phloroglucinol moiety in Hyp1 also resulted in an inactive compound (Hyp4). In previous studies, hyperforin was modified by acylation, alkylation, and oxidation, leading to a series of hyperforin analogs that were subsequently used to study structure-activity relationships (Verotta et al., 2002). All of these compounds were less potent inhibitors of synaptosomal serotonin reuptake than the parental compound, indicating a specific role for the enolized β-diketone moiety. The same was true for the synthesized phloroglucinols examined, suggesting that a covalent block of the tautomeric equilibrium by oxidation is detrimental for pharmacological activity.

Our modeling studies of possible ligand binding modes suggest that hyperforin, DAG, and the active hyperforin-like phloroglucinol derivatives have similar pharmacophoric characteristics. The definition of these interactions originated from a crystal structure of PXR in complex with hyperforin and provided the basis for the prediction of a probable three-dimensional conformation of the ligands, which would satisfy comparable hydrogen bonds, as observed in the complex structure. The computed preferred "down" conformation of hyperforin and the active derivatives is supported by our experimental findings and indicates that both carbonyl groups of the derivatives are essential for activity. This binding mode could also explain the inactivity of Hyp2 and Hyp6. The selectivity of hyperforin and

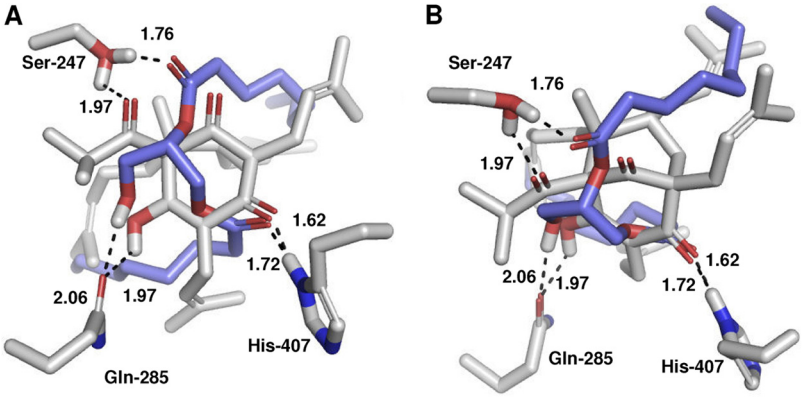

Fig. 7. Binding pocket of the human PXR in complex with hyperforin (Protein Data Bank identifier 1m13, white) and a docked conformation of DAG (blue). Shown are different views (A and B) of the model highlighting potentially relevant contact points. The interacting residues and both ligands are shown in stick representation (picture generated using Pymol). Hydrogen bonds are indicated by dashed lines, and the distances between hydrogen and their acceptor atoms are calculated in angstroms. Atom coordinates of Ser247 and Gln285 are identical with the PXR structure. The position of hydrogen from Ser247 binding to DAG were changed during docking to optimize hydrogen bond geometry; therefore, both hydrogen positions are visualized.

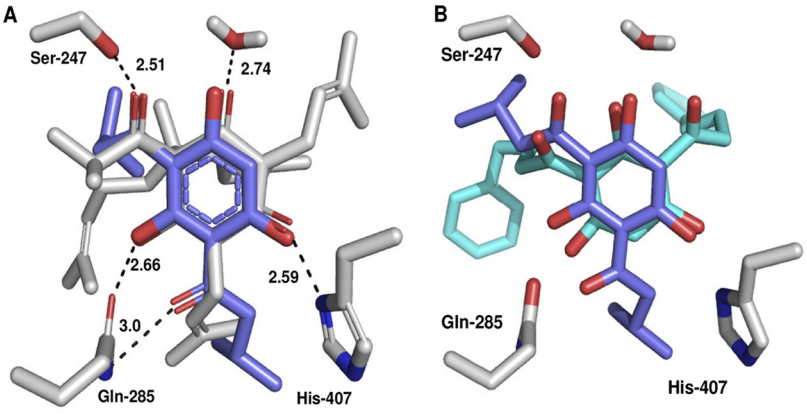

Fig. 8. Crystal structure of human pregnane X receptor binding domain in complex with hyperforin, Hyp1, and Hyp7. Crystal structure of the human pregnane X receptor binding domain in complex with hyperforin (Protein Data Bank identifier 1m13, white) and an aligned conformation (flexible pharmacophore alignment) of Hyp1 (blue) (A). Docking conformation proposed for Hyp1 (dark blue, "down") and Hyp7 (light blue, "up") (B). Interacting residues and both ligands are shown in stick representation (picture generated using Pymol). Hydrogen bonds are indicated by dashed lines, and distances between hydrogen bond donor and acceptor atoms are calculated in angstroms.

the symmetric 2,4-diacylphloroglucinols for TRPC6 might be due to the rigid structure of these compounds. In contrast, DAG is more flexible and might be able to interact with amino acids that are placed differently in TRPC3 and TRPC7 channels. The putative TRPC6 docking site of hyperforin in comparison with the PXR binding pocket will support further steps in compound optimization.

In summary, several symmetric 2,4-diacylphloroglucinol derivatives are the first chemically simplified and stable molecules that share the pharmacological profile with hyperforin and are potent and selective TRPC6 activators. Based on the profile of the tested TRP channels, we currently can not exclude the possibility that hyperforin or the 2,4-diacylphloroglucinol derivatives are modulators of unknown nonselective cation channels. In contrast to previous studies that modified the complex hyperforin structure, e.g., by alkylation or oxidation, we were able to create simplified chemical lead structures with 2,4-diacylphloroglucinol moiety as the essential pharmacophore. This structural core is essential for activation of TRPC6 channels, which indirectly results in the inhibition of neurotransmitter uptake and stimulation of neuronal differentiation processes. Our modeling studies suggest that the natural TRPC6 activator DAG, hyperforin, and the symmetric 2,4-diacylphloroglucinol derivatives share common interaction points with the target protein. Further evaluation of the crystal structure of TRPC6 and the identification of the binding pocket of hyperforin or other endogenous ligands is urgently needed to provide more insight into the structure-activity relationship of phloroglucinol derivatives.

Acknowledgments

We especially thank Dr. Klaus Klessing, former head of the department of chemical research, Dr. Willmar Schwabe GmbH and Co. KG Pharmaceuticals, Karlsruhe, Germany, for the synthesis of the 2-acyl- and 2,4-diacylphloroglucinol derivatives, and Dr. Kirill Essin for initial patch-clamp experiments.

References

Beerhues L (2006) Hyperforin. *Phytochemistry* **67:**2201–2207.
Brauchi S, Orta G, Mascayano C, Salazar M, Raddatz N, Urbina H, Rosenmann E, Gonzalez-Nilo F, and Latorre R (2007) Dissection of the components for PIP2 activation and thermosensation in TRP channels. *Proc Natl Acad Sci U S A* **104:**10246–10251.
Dietrich A and Gudermann T (2007) TRPC6. *Handb Exp Pharmacol* **179:**125–141.
Estacion M, Li S, Sinkins WG, Gosling M, Bahra P, Poll C, Westwick J, and Schilling WP (2004) Activation of human TRPC6 channels by receptor stimulation. *J Biol Chem* **279:**22047–22056.
Hofmann T, Obukhov AG, Schaefer M, Harteneck C, Gudermann T, and Schultz G (1999) Direct activation of human TRPC6 and TRPC3 channels by diacylglycerol. *Nature* **397:**259–263.
Jardín I, Redondo PC, Salido GM, and Rosado JA (2008) Phosphatidylinositol 4,5-bisphosphate enhances store-operated calcium entry through hTRPC6 channel in human platelets. *Biochim Biophys Acta* **1783:**84–97.
Jia Y, Zhou J, Tai Y, and Wang Y (2007) TRPC channels promote cerebellar granule neuron survival. *Nat Neurosci* **10:**559–567.
Jones G, Willett P, and Glen RC (1995) Molecular recognition of receptor sites using a genetic algorithm with a description of desolvation. *J Mol Biol* **245:**43–53.
Kwon Y, Hofmann T, and Montell C (2007) Integration of phosphoinositide- and calmodulin-mediated regulation of TRPC6. *Mol Cell* **25:**491–503.
Lemonnier L, Trebak M, and Putney JW Jr (2008) Complex regulation of the TRPC3, 6 and 7 channel subfamily by diacylglycerol and phosphatidylinositol-4,5-bisphosphate. *Cell Calcium* **43:**506–514.
Leuner K, Kazanski V, Müller M, Essin K, Henke B, Gollasch M, Harteneck C, and Müller WE (2007) Hyperforin–a key constituent of St. John's wort specifically activates TRPC6 channels. *FASEB J* **21:**4101–4111.
Li Y, Jia YC, Cui K, Li N, Zheng ZY, Wang YZ, and Yuan XB (2005) Essential role of TRPC channels in the guidance of nerve growth cones by brain-derived neurotrophic factor. *Nature* **434:**894–898.
Linde K, Berner MM, and Kriston L (2008) St John's wort for major depression. *Cochrane Database Syst Rev* **4:**CD000448.
Lovell SC, Davis IW, Arendall WB 3rd, de Bakker PI, Word JM, Prisant MG, Richardson JS, and Richardson DC (2003) Structure validation by Calpha geometry: phi,psi and Cbeta deviation. *Proteins* **50:**437–450.
Mandadi S and Roufogalis BD (2008) ThermoTRP channels in nociceptors: taking a lead from capsaicin receptor TRPV1. *Curr Neuropharmacol* **6:**21–38.
Montell C (2005) The TRP superfamily of cation channels. *Sci STKE* **2005:**re3.
Montell C (2006) TRP channels: mediators of sensory signaling and roles in health and disease. *Chem Senses* **31:**A45.
Müller M, Essin K, Hill K, Beschmann H, Rubant S, Schempp CM, Gollasch M, Boehncke WH, Harteneck C, Müller WE, and Leuner K (2008) Specific TRPC6 channel activation, a novel approach to stimulate keratinocyte differentiation. *J Biol Chem* **283:**33942–54.
Müller WE (2003) Current St John's wort research from mode of action to clinical efficacy. *Pharmacol Res* **47:**101–109.
Nilius B, Owsianik G, and Voets T (2008) Transient receptor potential channels meet phosphoinositides. *EMBO J* **27:**2809–2816.
Singer A, Wonnemann M, and Müller WE (1999) Hyperforin, a major antidepressant constituent of St. John's Wort, inhibits serotonin uptake by elevating free intracellular Na^+. *J Pharmacol Exp Ther* **290:**1363–1368.
Smyth JT, Lemonnier L, Vazquez G, Bird GS, and Putney JW Jr (2006) Dissociation of regulated trafficking of TRPC3 channels to the plasma membrane from their activation by phospholipase C. *J Biol Chem* **281:**11712–11720.
Tada M, Chiba K, Takakuwa T, and Kojima E (1992) Analogues of natural phloroglucinols as antagonists against both thromboxane A2 and leukotriene D4. *J Med Chem* **35:**1209–1212.
Tai Y, Feng S, Ge R, Du W, Zhang X, He Z, and Wang Y (2008) TRPC6 channels promote dendritic growth via the CaMKIV-CREB pathway. *J Cell Sci* **121:**2301–2307.
Trebak M, St J Bird G, McKay RR, Birnbaumer L, and Putney JW Jr (2003) Signaling mechanism for receptor-activated canonical transient receptor potential 3 (TRPC3) channels. *J Biol Chem* **278:**16244–16252.
Treiber K, Singer A, Henke B, and Müller WE (2005) Hyperforin activates nonselective cation channels (NSCCs). *Br J Pharmacol* **145:**75–83.
Vazquez G, Wedel BJ, Kawasaki BT, Bird GS, and Putney JW Jr (2004) Obligatory role of Src kinase in the signaling mechanism for TRPC3 cation channels. *J Biol Chem* **279:**40521–40528.
Verotta L, Appendino G, Belloro E, Bianchi F, Sterner O, Lovati M, and Bombardelli E (2002) Synthesis and biological evaluation of hyperforin analogues. Part I. Modification of the enolized cyclohexanedione moiety. *J Nat Prod* **65:**433–438.
Verotta L, Appendino G, Belloro E, Jakupovic J, and Bombardelli E (1999) Furohyperforin, a prenylated phloroglucinol from st. John's wort (*Hypericumperforatum*). *J Nat Prod* **62:**770–772.
Verotta L, Appendino G, Jakupovic J, and Bombardelli E (2000) Hyperforin analogues from St. John's wort (*Hypericum perforatum*). *J Nat Prod* **63:**412–415.
Verotta L, Lovaglio E, Sterner O, Appendino G, and Bombardelli E (2004) Modulation of chemoselectivity by protein additives. Remarkable effects in the oxidation of hyperforin. *J Org Chem* **69:**7869–7874.
Voets T and Nilius B (2007) Modulation of TRPs by PIPs. *J Physiol* **582:**939–944.
Voets T, Talavera K, Owsianik G, and Nilius B (2005) Sensing with TRP channels. *Nat Chem Biol* **1:**85–92.
Watkins RE, Maglich JM, Moore LB, Wisely GB, Noble SM, Davis-Searles PR, Lambert MH, Kliewer SA, and Redinbo MR (2003) 2.1 A crystal structure of human PXR in complex with the St. John's wort compound hyperforin. *Biochemistry* **42:**1430–1438.
Wonnemann M, Singer A, and Müller WE (2000) Inhibition of synaptosomal uptake of ^{3}H-L-glutamate and 3H-GABA by hyperforin, a major constituent of St. John's Wort: the role of amiloride sensitive sodium conductive pathways. *Neuropsychopharmacology* **23:**188–197.
Zhou J, Du W, Zhou K, Tai Y, Yao H, Jia Y, Ding Y, and Wang Y (2008) Critical role of TRPC6 channels in the formation of excitatory synapses. *Nat Neurosci* **11:**741–743.

Address correspondence to: Dr. Kristina Leuner, Institute of Pharmacology, Goethe University, Biocenter N260 1. Floor, Max-von-Laue-Str. 9, 60438 Frankfurt, Germany. E-mail: leuner@em.uni-frankfurt.de.